

# Time-resolved imaging of electrical discharge development in underwater bubbles

Yalong Tu, Hualei Xia, Yong Yang,<sup>a)</sup> and Xinpei Lu<sup>a)</sup>

*State Key Laboratory of Advanced Electromagnetic Engineering and Technology, Huazhong University of Science and Technology, Wuhan, Hubei Province 430074, China*

(Received 23 November 2015; accepted 28 December 2015; published online 11 January 2016)

The formation and development of plasma in single air bubbles submerged in water were investigated. The difference in the discharge dynamics and the after-effects on the bubble were investigated using a 900 000 frame per second high-speed charge-coupled device camera. It was observed that depending on the position of the electrodes, the breakdown could be categorized into two modes: (1) direct discharge mode, where the high voltage and ground electrodes were in contact with the bubble, and the streamer would follow the shortest path and propagate along the axis of the bubble and (2) dielectric barrier mode, where the ground electrode was not in touch with the bubble surface, and the streamer would form along the inner surface of the bubble. The oscillation of the bubble and the development of instabilities on the bubble surface were also discussed.

© 2016 AIP Publishing LLC. [<http://dx.doi.org/10.1063/1.4939704>]

## I. INTRODUCTION

Discharges in gas phase have been extensively studied and used in industry for over 100 years. In comparison, plasma in or in contact with water is a relatively new field, which has fast development during recent years.<sup>1–3</sup> The simultaneous production of high energy radicals, ions, molecular species, UV radiation, and shock waves by underwater discharges makes them suitable for a wide range of applications such as water sterilization, volatile organic compounds (VOCs) removal, nanomaterial synthesis, and ultrasound generation.<sup>4–8</sup>

Generally, electrical breakdown in water requires much higher electric field than in gas, due to the fact that the density of water is approximately 1000 times higher than that of atmospheric gas. The increase of electric field means the increase in voltage or decrease in radius at needle electrode tip (for pin-pin or pin-plane electrode system). However, higher voltage means higher cost for power supply and higher requirement for electrical insulation, while sharper needle electrode means easier erosion and subsequently higher cost for maintenance. One alternative is to introduce gas bubbles during the breakdown process.<sup>9–12</sup> The presence of bubbles between submerged electrodes significantly reduces electric field required, resulting in a significant reduction of breakdown voltage to the level which is only slightly higher than those required in gas state. Additionally, plasma discharge in bubbles is attractive for applications where the plasma–liquid interface is preferred to be as large as possible. This feature is usually desired in most water treatment applications as it promotes the diffusion of reactive species into liquid water.

Under such context, it is important to obtain a better understanding of the fundamental discharge streamer behavior and their development in bubble filled liquids.<sup>13–15</sup>

Optical emission spectroscopy (OES) and high-speed photography are the two major non-intrusive tools utilized in the diagnosis of the underwater breakdown. Current time-resolved observations using these tools usually rely on the technique to adjust the delay time of the intensified charge-coupled device (ICCD) camera, to capture the snapshots of successive breakdown events at their different development stage. These snapshots of different breakdown events are then sorted and put together at the correct time order to represent the dynamics of the discharge.<sup>16</sup> Satisfactory results have been obtained using this technique for gas phase discharges, where the repeatability of the gas breakdown process is relatively good. However, this technique is limited by the shot-to-shot instability of the underwater discharge, originating from the stochastic nature of the breakdown processes in both light emission intensity and plasma structure. The focus of the current paper is to investigate the formation and development of plasma in an isolated gas bubble submerged in water during single breakdown event. With the utilization of ultra-speed camera (approximately  $10^6$  frames per second), single events could be followed from initiation to extinction to eliminate the stochastic behavior of the discharge.

## II. EXPERIMENTAL SETUP

The front and top views of the experimental setup are shown in Figs. 1(a) and 1(b), respectively. Air bubbles were introduced into water through a quartz tube. The inner diameter of the tube was  $100\ \mu\text{m}$ , and the outer diameter of the tube was  $300\ \mu\text{m}$ . The quartz tube was connected to a microsyringe. By regulating the input gas volume from the microsyringe, the diameter of the bubble (shown in Fig. 1(a) as  $D$ ) formed at the top of the quartz tube could be easily controlled. The vertical position of the quartz tube, and thus the vertical position of the air bubble, could be adjusted using a micrometer caliper connected from the bottom of the tube.

<sup>a)</sup>Authors to whom correspondence should be addressed. Electronic addresses: yangyong@hust.edu.cn and luxinpei@hust.edu.cn.

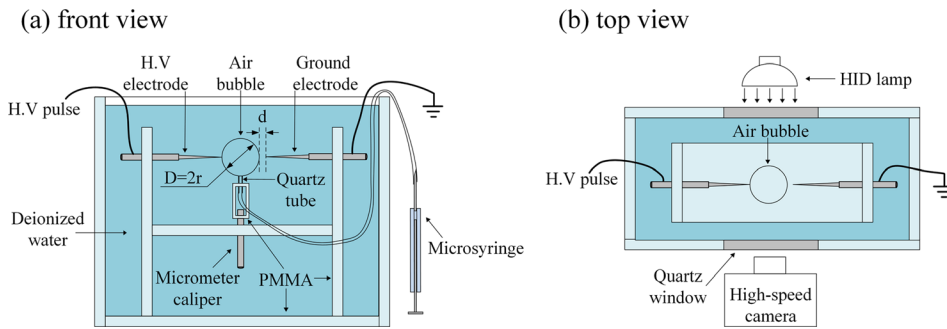


FIG. 1. Schematic of the experimental setup: (a) front view and (b) top view.

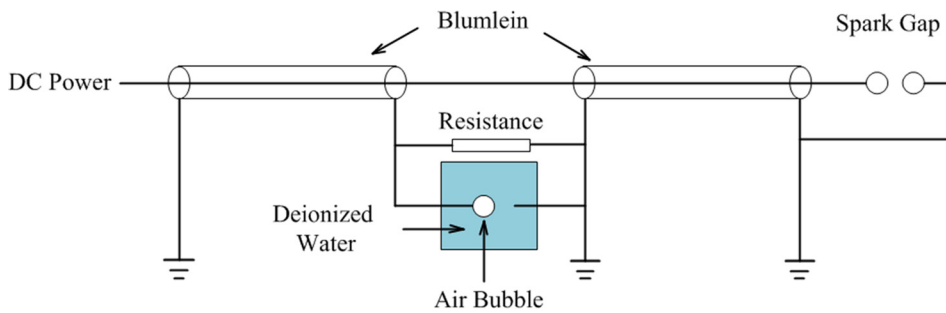


FIG. 2. Schematic diagram of the Blumlein generator. The matching resistance was  $150\ \Omega$ . The spark gap was triggered manually to produce single electric pulse.

Two stainless steel pin electrodes were used to produce plasma inside the bubble. One electrode was connected to the high voltage, and the other was connected to the ground. The horizontal position of these two electrodes could be independently adjusted using another two micrometer calipers. These two calipers, along with the other one attached to the bottom of the quartz tube, enabled the two-dimensional movement of air bubble relative to the pin-to-pin electrode system. In our current experiment, the high voltage electrode was maintained in contact with the gas bubble, while the distance between the ground electrode and the right side of the air bubble (shown in Fig. 1(a) as  $d$ ) was varied. The entire setup was submerged in de-ionized water, whose conductivity and pH value were measured to be  $0.3\ \mu\text{S}/\text{cm}$  and 7.0, respectively. The gas used in current experiment was air.

A Blumlein generator, with a matching resistance of  $150\ \Omega$ , was used as the pulse power source (as shown in Fig. 2). The pulse was triggered using a manual switch on a single discharge basis. A voltage probe divider (Tektronix P6015) was used to measure the voltage on the electrode. The electric signal was recorded by a Tektronix DPO7104 wideband digital oscilloscope. Figure 3 shows the measured waveform of the voltage power source. The peak voltage was  $+30\ \text{kV}$ . The rise time of the pulse was about 40 ns, and the full width at half maximum (FWHM) of the pulse was about 100 ns.

The dynamics of the plasma inside the bubble was recorded by a high-speed camera (Photron FASTCAM SA Z) with a frame rate of 900 000 per second at free run mode. The exposure time of each image was 197 ns. To get clear, no excessive-exposure pictures, a high intensity discharge (HID) lamp was used to illuminate the discharge area from the back.

### III. RESULTS AND DISCUSSIONS

Discharge created in the bubble behaves differently according to a number of parameters, including the applied

voltage, electrode configuration, water conductivity, and gas composition. From the experiments, it was observed that the dynamics of the discharge could be very different when the relative position of electrodes to the gas bubble was different. So the influence of electrode's vertical and horizontal positions on the discharge formation and development were first investigated.

#### A. Influence of electrode's vertical positions

Figure 4(a) shows the appearance of the discharge when both the electrodes were perfectly aligned with the center of the bubble. The exposure time of all images was set at 197 ns, which was the minimum value allowed by the camera. No strong filamentation was observed inside the bubble. The discharge propagated along the upper and lower surfaces of the bubble wall and formed a complete circle around the inner surface. This was probably due to the strong refraction of the electric field along the gas-liquid interface, as predicted by the

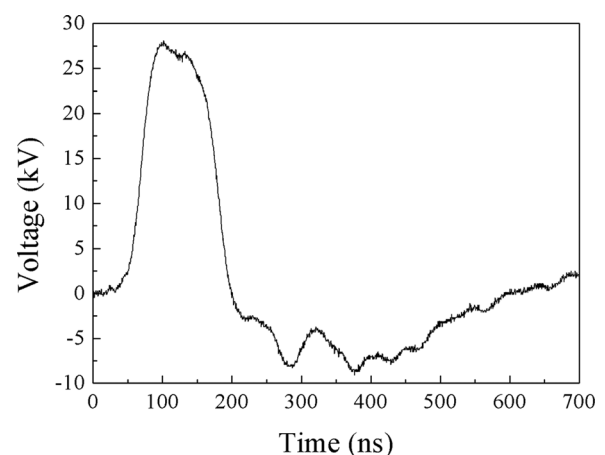


FIG. 3. Voltage waveform produced by the Blumlein generator.

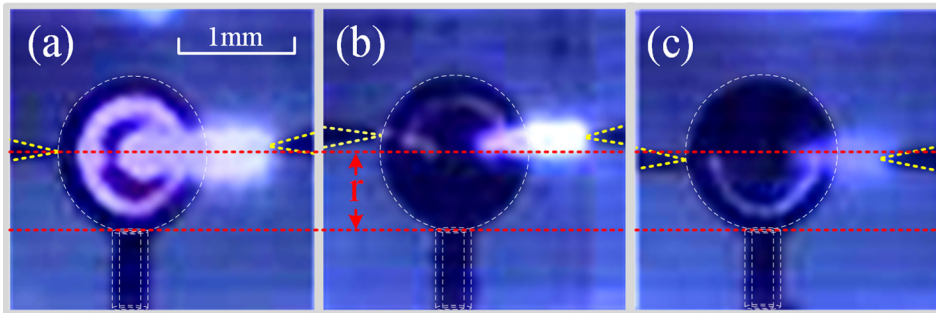


FIG. 4. Influence of electrodes' vertical position to discharge appearance: (a) if the electrodes were perfectly aligned with the center of the bubble, the discharge would propagate along the upper and lower surfaces of the bubble wall and formed a complete circle around the inner surface; if the electrodes were shifted above (b) or below (c) the centerline, the discharge would propagate only along the upper or lower surface of the bubble.

numerical simulations.<sup>17,18</sup> This phenomenon could also be explained by the higher concentration of water vapor close to the air-liquid interface. The ionization coefficient of water vapor is significantly higher than that of air. Thus, a local increase in the water vapor pressure would facilitate plasma formation. However, the phenomenon was not necessarily correlated to the higher  $\text{H}_2\text{O}$  vapor density near the interface, as studies indicated that the surface-propagating discharges also occurred in pure, dry gases.<sup>17</sup> Obviously, the propagation of the streamers along the surface was beneficial for most water treatment applications, as the resulting reactive species will be in direct contact with the liquid, leading to a more effective treatment of the liquid medium.

Additionally, it was observed that the formation of the surface discharge was influenced by the vertical position of the electrode. If the electrodes were shifted slightly above the centerline of the bubble, the streamer would only propagate along the upper surface of the bubble (as shown in Fig. 4(b)). Similar effects were observed when the electrode was shifted below the centerline of the bubble, as shown in Fig. 4(c). Here, the bubble plasma was essentially a surface dielectric barrier discharge (DBD). Charge accumulated on the surface of the interface, which provided the functionality of a dielectric barrier discharge.

## B. Influence of electrode's horizontal position

In this part, the influence of electrode's horizontal positions on the discharge dynamics was investigated. Figure 5 shows the development of the breakdown process inside the bubble when both electrodes were in contact with the bubble ( $d = 0 \mu\text{m}$ ). In this case, the discharge behaved similarly to the breakdown process in gas phase, where the streamer was connected to the high voltage electrode and the ground electrode through the shortest path, i.e., along the axis of the bubble (we call it "direct discharge" mode). Although the FWHM of the high voltage pulse was about 100 ns, the lifetime of the bubble plasma was in the order of several microseconds. When the conductive channel bridged the gap, a significant increase of light emission was observed at  $1 \mu\text{s}$ . After that, the streamer expanded and filled the entire void. The intensity of the discharge started to drop after about  $2 \mu\text{s}$  and extinguished within  $6 \mu\text{s}$ .

As shown in Fig. 6, when the ground electrode was not in direct contact with the bubble, a gas phase plasma would form along the inner surface of the bubble. As discussed previously, the so-called "surface-hugging" plasma<sup>17</sup> was essentially a dielectric barrier discharge. When the discharge initiated inside the bubble, charges would accumulate on the inner surface of the bubble with the incident plasma flux. For

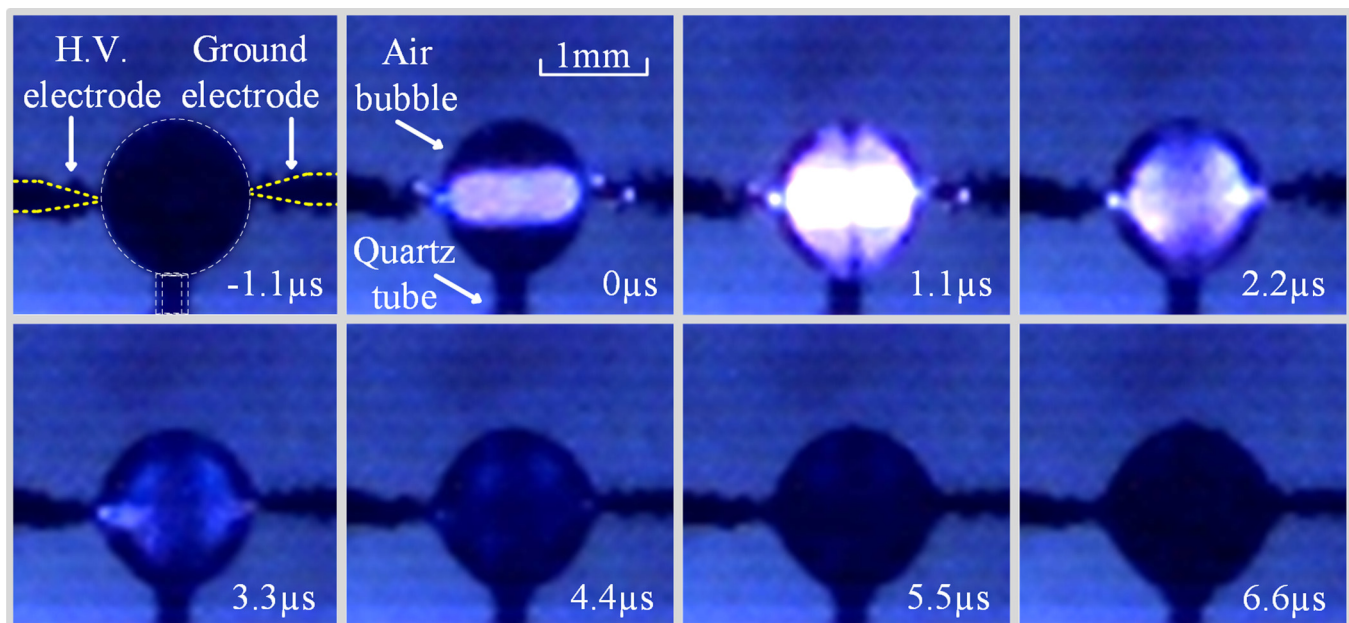


FIG. 5. Dynamic process of discharge when both the high voltage and ground electrodes were in contact with the bubble ( $d = 0 \mu\text{m}$ ).

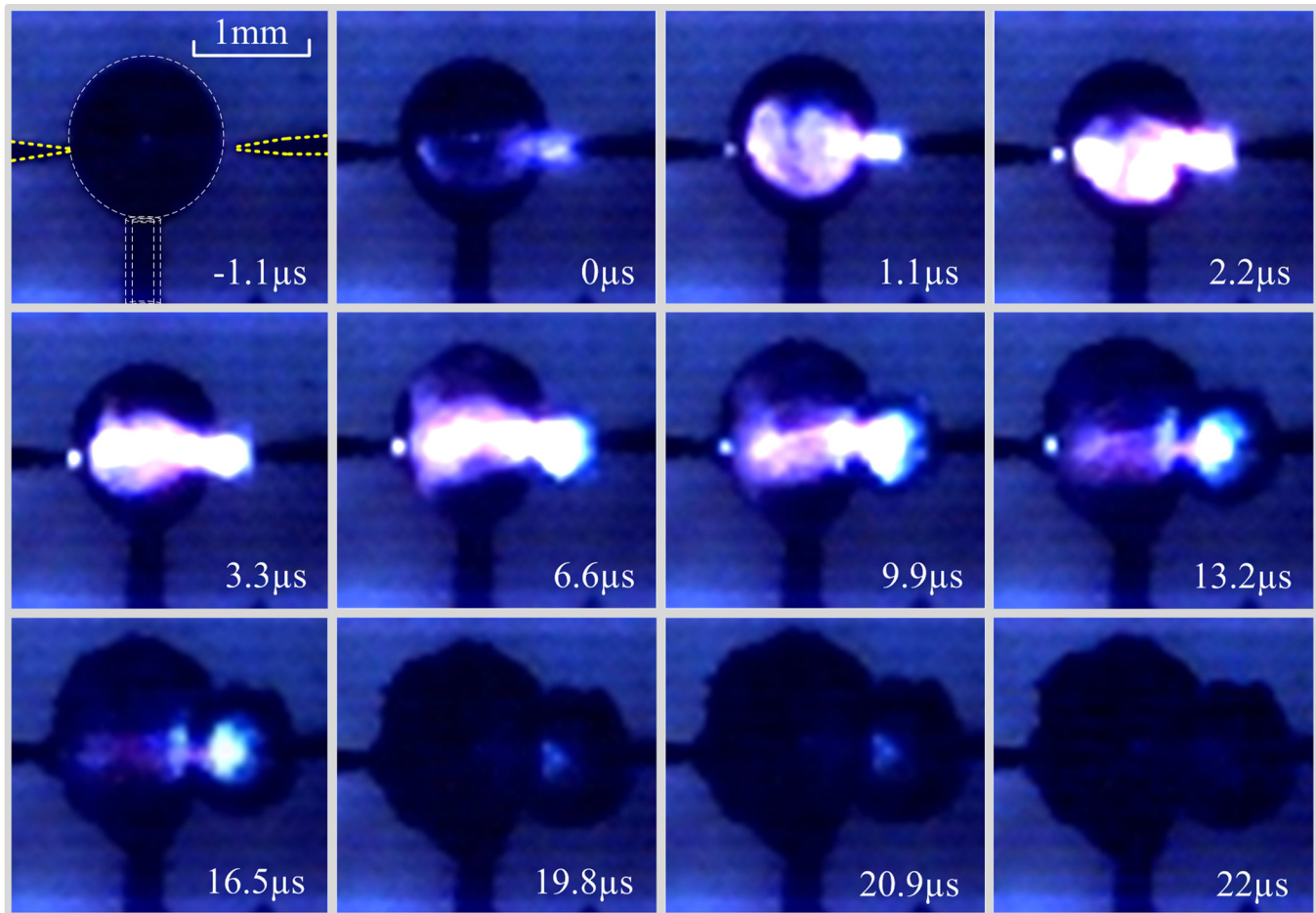


FIG. 6. Dynamic process of discharge when the ground electrode was not in contact with the bubble ( $d = 50 \mu\text{m}$ ).

our experiment, the dielectric relaxation time was in the order of  $10 \mu\text{s}$ . If we assume a typical streamer propagation velocity of  $10^5$ – $10^6$  m/s, the time required for plasma initiation would be in the order of a few nanoseconds. So the accumulation of charge inside the bubble was a relatively good approximation at the early stage of plasma development. Here, we cannot see the bridging process of the streamer over the electrode gap, since the gate time of our current experiment setup was at least 1 order of magnitude longer than that of plasma initiation time. Numerical simulations performed by Tian *et al.* showed that the discharge started at the tip of the high-voltage electrode and propagated towards the opposite side of the bubble surface.<sup>17</sup> Another thing worth noting was that the peak current of the “surface-hugging” mode (or “dielectric barrier” mode) was 2–3 times lower than that of the “direct discharge” mode, possibly due to the existence of water barrier.

For conventional DBDs, the discharge is terminated when charge accumulates at the surface of the dielectric. However, this was not the case in our underwater bubble breakdown experiments. A secondary streamer would initiate at the tip of the ground electrode, which was immersed in liquid water. Again, due to the limitation of our current setup, it was not possible to tell whether the secondary streamer was initiated directly by the electric field at the tip of the ground electrode or due to the injection and accumulation of charge on the gas-liquid interface by the “surface-hugging” streamer. The plasma

generated at these two different locations would connect with each other and form a conductive path between the two electrodes, resulting in a dramatic increase in light emission. As shown in Figs. 6 and 7, when the value of  $d$  (the distance between the ground electrode and the bubble) increased, the overall intensity of the plasma decreased. After the bridging stage, the plasma inside bubble became more diffuse and expanded to occupy part of the bubble. Numerical simulation by Tian *et al.* showed that the temperature of electrons was about 8–10 eV.<sup>17</sup> Part of these electrons would deposit on the gas-liquid interface and screen out the electric field into the water. Other part of the electrons would penetrate into the bubble. These high energy electrons were capable of causing direct impact excitation of ground state H/OH and dissociative excitation of  $\text{H}_2\text{O}$ , leading to the OH(A-X) and  $\text{H}_\alpha$  emission in the visible light range. The penetration depth was limited by the electron energy relaxation length in humid air. The relaxation length was typically smaller than the size of the gas bubble, so the plasma was not able to fill the entire bubble. At around  $2 \mu\text{s}$ , a secondary bubble would appear at the tip of the ground electrode and expanded with time, possibly due to the joule heating caused by the ionic current in water.

When the value of  $d$  further increased, i.e., the ground electrode was further retracted from the bubble, it became more difficult to initiate plasma in both the bubble and water. As shown in Fig. 8, for the case of  $d = 350 \mu\text{m}$ , the discharge initiated at  $0 \mu\text{s}$ , followed by a quick relaxation of plasma

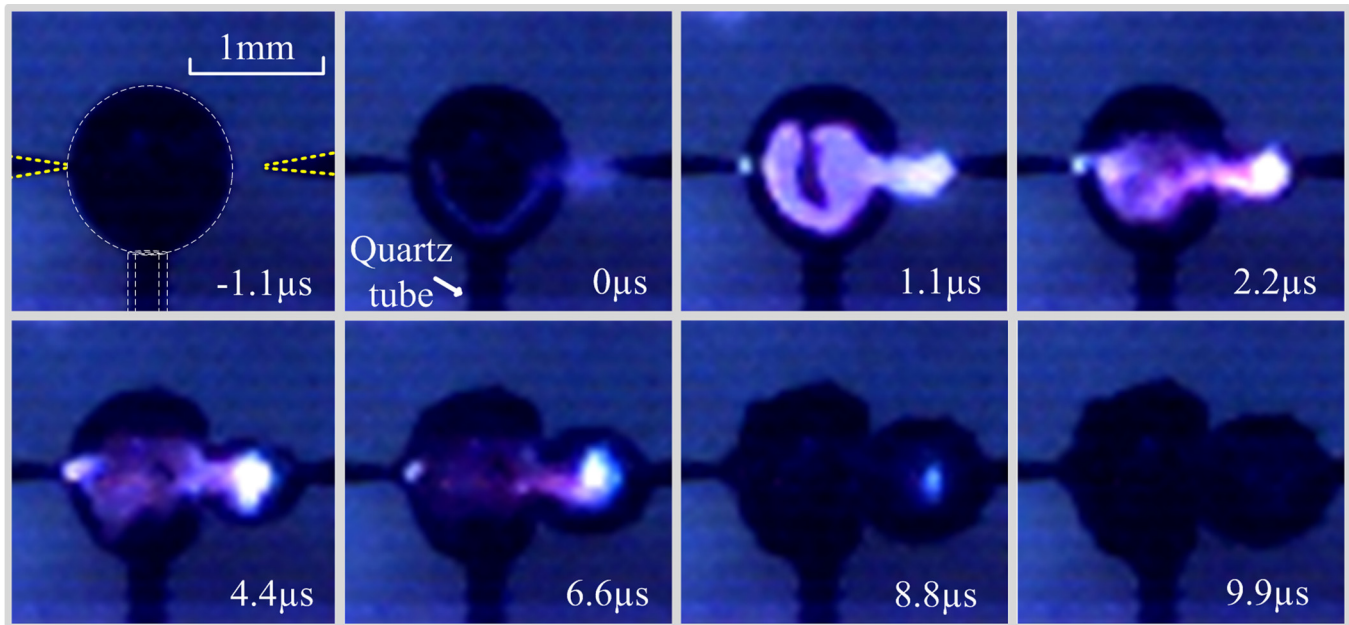


FIG. 7. Dynamic process of discharge when the ground electrode was not in contact with the bubble ( $d = 200 \mu\text{m}$ ).

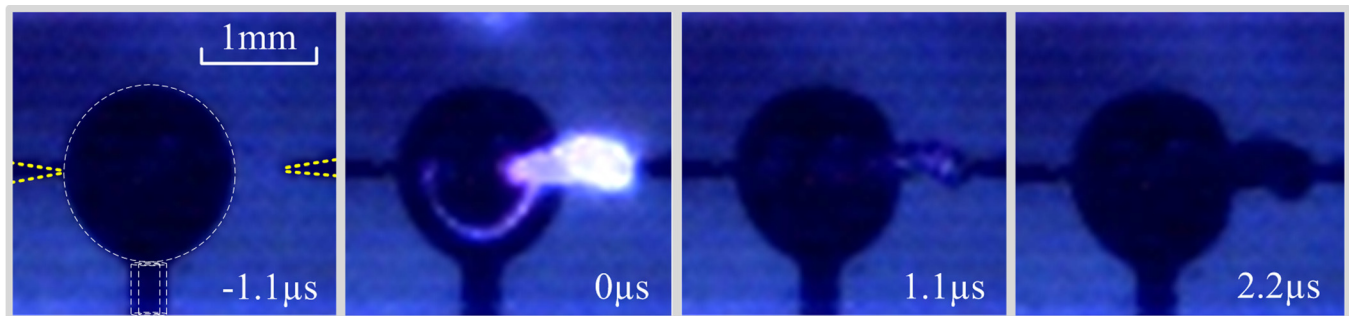


FIG. 8. Dynamic process of discharge when the ground electrode was not in contact with the bubble ( $d = 350 \mu\text{m}$ ).

within  $2 \mu\text{s}$ . For  $d$  values greater than  $500 \mu\text{m}$ , no plasma formation was observed at the same voltage level.

From results presented above, one thing worth noting was that although the FWHM of the high voltage pulse was only about  $100 \text{ ns}$ , the duration of plasma inside the bubble (defined as the time with light emission) was well beyond that time range. Figure 9 shows the plasma duration time as a function of  $d$ . It was clear from the figure that as the distance between ground electrode and gas bubble increased from  $50 \mu\text{m}$  to  $450 \mu\text{m}$ , the duration time decreased from  $24 \mu\text{s}$  to less than  $4 \mu\text{s}$ . This trend coincided with the fact that when the ground electrode was not in contact with the bubble, the duration time of the residual current decreased as the value of  $d$  increased. From Fig. 10, it could be seen that the current comprised two parts: the sinusoidal oscillation part and the long decaying tail part. Both parts were exponentially damped. The sinusoidal oscillation had a frequency of about  $2 \text{ MHz}$  for all cases, which corresponded to the ringing frequency of the voltage. The decaying tail current was probably caused by the dielectric relaxation of the accumulated charges on the gas-liquid interface, since the time constant  $\tau$  for the decaying tail was about  $10 \mu\text{s}$ , which was in the same range with the dielectric relaxation time.

From the energy point of view, the difference in plasma duration time was possibly associated with different energy levels injected into the bubble during the breakdown process. Indeed, this explanation was supported by the energy consumption calculation. By integrating the product of the voltage

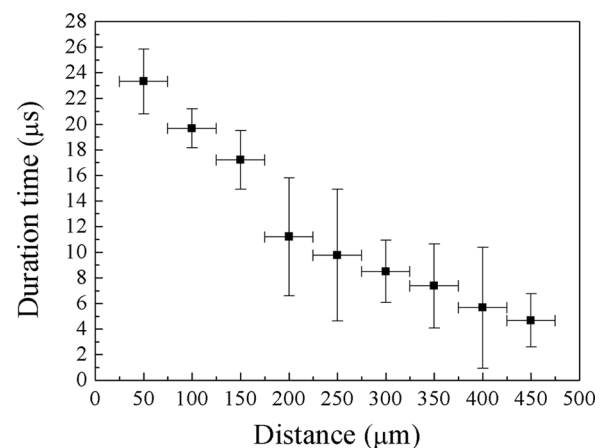


FIG. 9. The duration of plasma inside the bubble versus the distance between the ground electrode and the bubble.

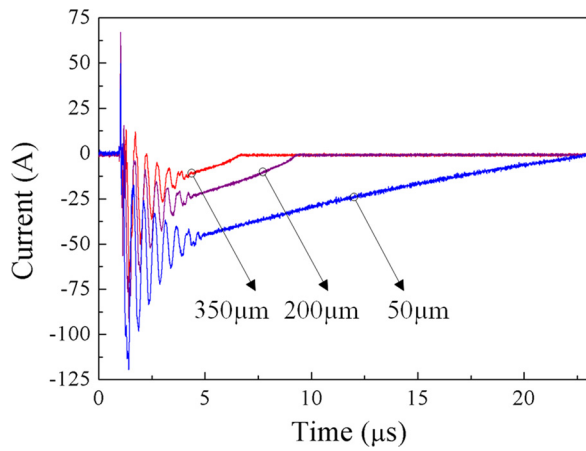


FIG. 10. Waveforms of discharge currents for  $d = 50, 200,$  and  $350 \mu\text{m}$ . The current comprised two parts: the sinusoidal oscillation part and the long decaying tail part.

and current, it is shown that the total energy injection into the bubble per breakdown decreased from  $0.55 \text{ J}$  to  $0.15 \text{ J}$ , as the ground electrode was retracted from the bubble (from  $d = 50 \mu\text{m}$  to  $d = 450 \mu\text{m}$ ) (Fig. 11). The bubble-water-electrode system was capacitively coupled. When the ground electrode was retracted away from the bubble, it was essentially

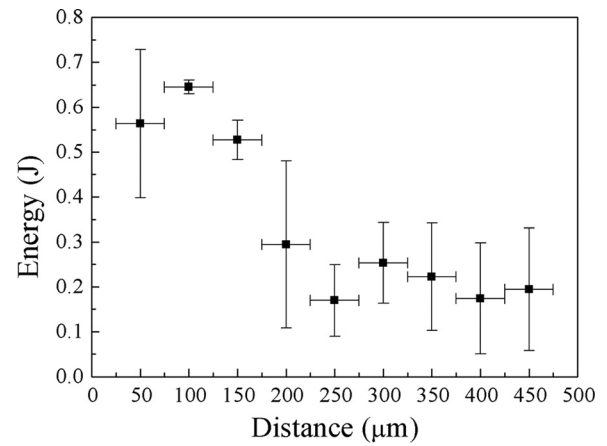


FIG. 11. Energy injection into the bubble per breakdown versus  $d$ .

increasing the thickness of dielectric in the capacitor, resulting in a decrease in the capacitance. As a result, as the value of  $d$  increased, the capacitance decreased, leading to a decrease in the injected energy. When the distance was larger than the threshold value (for our case,  $500 \mu\text{m}$ ), the injected energy was not sufficient to initiate the breakdown process, so no plasma could be observed.

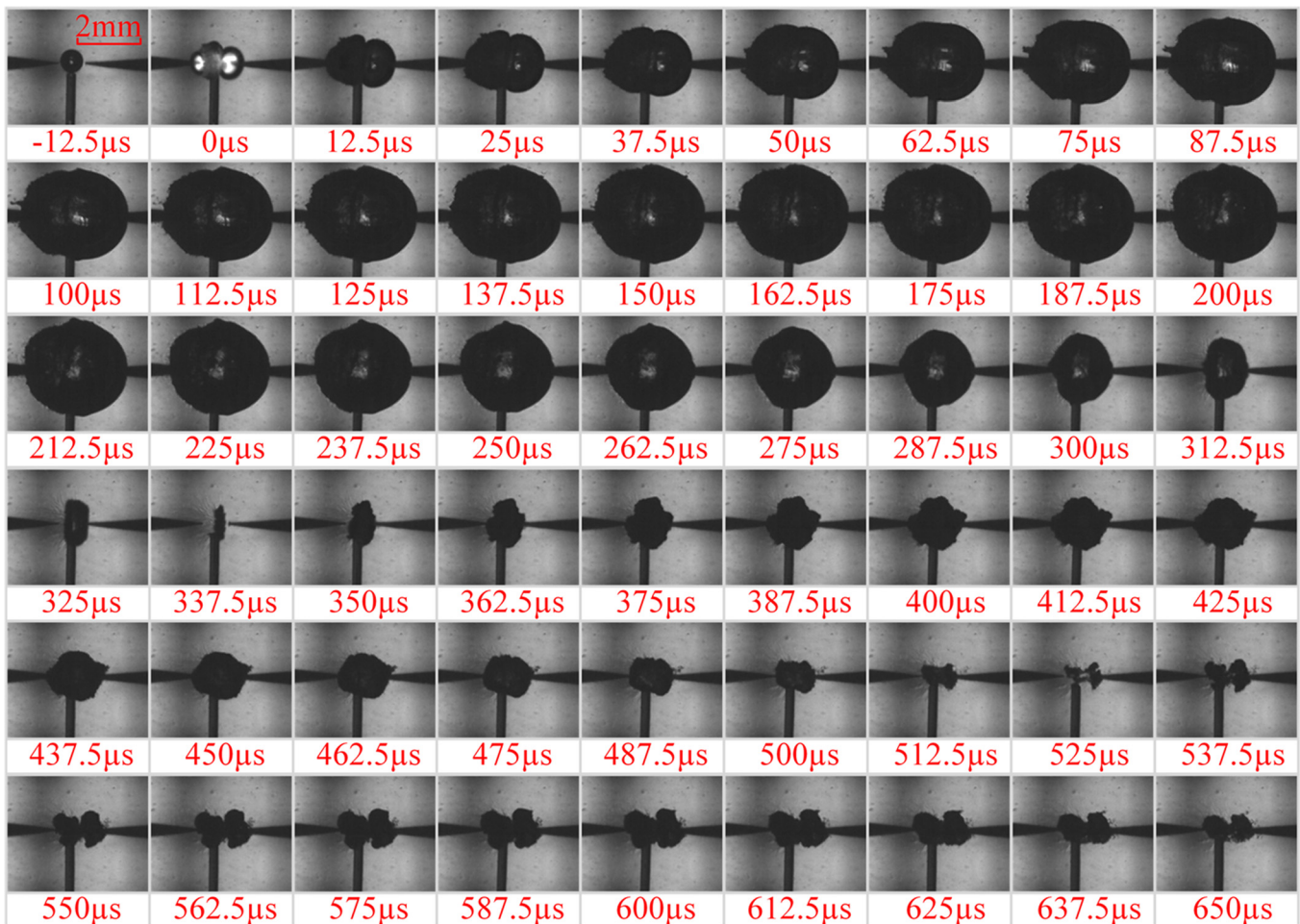


FIG. 12. Time-sequence photos of the breakdown process in underwater air bubble using a high speed CCD camera running at a frame rate of 80 000 per second.

### C. Post discharge bubble oscillation

Figure 12 shows a sequence of 54 frames corresponding to generation of the discharge and subsequent hydrodynamic oscillation of the bubble. The images were taken at a frame rate of 80 000 per second with 197 ns exposure time. The lifetime of the discharge and its afterglow was significantly shorter than the time scale of the bubble growth. So light emission was observed only in the second frame. The white dot at the center of the bubble corresponds to the image of the backlight. The fast injection of electrical energy induced sudden increase in temperature and pressure both inside the bubble and the streamer connecting the ground electrode and the bubble. As a result, a secondary bubble was formed at the position of the streamer and merged with the pre-existing bubble. The combined bubble was seen to grow, reaching a maximum diameter of about 5 mm after 150  $\mu$ s, and then collapse to a minimum diameter of less than 0.5 mm at around 337.5  $\mu$ s, and continue to grow and collapse in several decaying oscillations. The whole process lasted around 700  $\mu$ s. The oscillation of the spherical microbubble could be described using the Rayleigh-Plesset (RP) model.<sup>19,20</sup> During the oscillation process, the bubble surface was distorted and no longer exhibited spherical shape. This was probably caused by the charge deposition of the streamer on the surface of the bubble, causing repulsion of the surface elements. Jetting of the gas bubble was observed at the first growing stage, as small protrusion appeared and grew from the right side of the bubble surface during 37.5  $\mu$ s to 100  $\mu$ s. The instability became larger as the bubble was deformed from its spherical shape during the subsequent oscillations, finally leading to the collapse of the bubble.

### IV. CONCLUSIONS

The introduction of bubble offers a pathway for generation of underwater plasma at a reduced electric field. The breakdown process of these bubbles, however, remains not fully understood. In this paper, the formation and propagation of plasma in gas bubble submerged in water during one single breakdown event were investigated. It was observed that the breakdown could be categorized into two modes: (1) direct discharge mode, where the high voltage and ground electrodes were in contact with the bubble, and the discharge behaved similarly to those in gas phase and the streamer would follow the shortest path and propagate along the axis of the bubble; (2) dielectric barrier mode, where the ground electrode was retracted from the bubble surface and the streamer would form both in the bubble and in liquid water. The plasma inside the bubble was initially confined to the bubble's inner surface and later diffused to fill the rest of the bubble. Energy calculation showed that the inject energy decreased as the distance between the ground electrode and the bubble increased. A threshold distance existed to ensure the breakdown of the bubble. The breakdown process was followed by the oscillation of the bubble, which led to the development of instability on the surface of the bubble. The

instability was possibly caused by the accumulation of charge on the gas-liquid interface. Future work will focus on the mechanism for the mass and energy transfer at the interface.

### ACKNOWLEDGMENTS

This work was supported by the National Natural Science Foundation of China under Grant Nos. 51077063, 51277087, 51477066, 11205065, and 51577080.

- <sup>1</sup>P. Bruggeman and C. Leys, "Non-thermal plasmas in and in contact with liquids," *J. Phys. D: Appl. Phys.* **42**(5), 053001 (2009).
- <sup>2</sup>B. Locke, J.-S. Chang, M. Sato, M. Hoffmann, and P. Sunka, "Electrohydraulic discharge and nonthermal plasma for water treatment," *Indus. Eng. Chem. Res.* **45**(3), 882–905 (2006).
- <sup>3</sup>Y. Yang, Y. I. Cho, and A. Fridman, *Plasma Discharge in Liquid: Water Treatment and Applications* (CRC Press, 2012).
- <sup>4</sup>B. Locke and S. Thagard, "Analysis and review of chemical reactions and transport processes in pulsed electrical discharge plasma formed directly in liquid water," *Plasma Chem. Plasma Process* **32**(5), 875–917 (2012).
- <sup>5</sup>H. Akiyama, "Streamer discharges in liquids and their applications," *IEEE Trans. Dielectr. Electr. Insul.* **7**(5), 646–653 (2000).
- <sup>6</sup>B. R. Locke and K.-Y. Shih, "Review of the methods to form hydrogen peroxide in electrical discharge plasma with liquid water," *Plasma Sources Sci. Technol.* **20**(3), 034006 (2011).
- <sup>7</sup>H. Xia and Y. Yang, "Note: Liquid chemical sensing by emission spectroscopy with a nanosecond pin-hole discharge in water," *Rev. Sci. Instrum.* **86**(1), 016101 (2015).
- <sup>8</sup>Y. Yang, H. Kim, A. Starikovskiy, Y. I. Cho, and A. Fridman, "Note: An underwater multi-channel plasma array for water sterilization," *Rev. Sci. Instrum.* **82**(9), 096103 (2011).
- <sup>9</sup>K.-Y. Shih and B. Locke, "Chemical and physical characteristics of pulsed electrical discharge within gas bubbles in aqueous solutions," *Plasma Chem. Plasma Process* **30**(1), 1–20 (2010).
- <sup>10</sup>H. Aoki, K. Kitano, and S. Hamaguchi, "Plasma generation inside externally supplied Ar bubbles in water," *Plasma Sources Sci. Technol.* **17**(2), 025006 (2008).
- <sup>11</sup>P. Bruggeman, C. Leys, and J. Vierendeels, "Electrical breakdown of a bubble in a water-filled capillary," *J. Appl. Phys.* **99**(11), 116101 (2006).
- <sup>12</sup>P. Vanraes, A. Nikiforov, and C. Leys, "Electrical and spectroscopic characterization of underwater plasma discharge inside rising gas bubbles," *J. Phys. D: Appl. Phys.* **45**(24), 245206 (2012).
- <sup>13</sup>B. Sommers, J. Foster, N. Y. Babaeva, and M. J. Kushner, "Observations of electric discharge streamer propagation and capillary oscillations on the surface of air bubbles in water," *J. Phys. D: Appl. Phys.* **44**(8), 082001 (2011).
- <sup>14</sup>K. Tachibana, Y. Takekata, Y. Mizumoto, H. Motomura, and M. Jinno, "Analysis of a pulsed discharge within single bubbles in water under synchronized conditions," *Plasma Sources Sci. Technol.* **20**(3), 034005 (2011).
- <sup>15</sup>B. Sommers and J. Foster, "Plasma formation in underwater gas bubbles," *Plasma Sources Sci. Technol.* **23**(1), 015020 (2014).
- <sup>16</sup>A. Hamdan, I. Marinov, A. Rousseau, and T. Belmonte, "Time-resolved imaging of nanosecond-pulsed micro-discharges in heptane," *J. Phys. D: Appl. Phys.* **47**(5), 055203 (2014).
- <sup>17</sup>W. Tian, K. Tachibana, and M. J. Kushner, "Plasmas sustained in bubbles in water: optical emission and excitation mechanisms," *J. Phys. D: Appl. Phys.* **47**(5), 055202 (2014).
- <sup>18</sup>N. Y. Babaeva and M. J. Kushner, "Structure of positive streamers inside gaseous bubbles immersed in liquids," *J. Phys. D: Appl. Phys.* **42**(13), 132003 (2009).
- <sup>19</sup>P. Xiao and D. Staack, "Microbubble generation by microplasma in water," *J. Phys. D: Appl. Phys.* **47**(35), 355203 (2014).
- <sup>20</sup>X. Lu, "One-dimensional bubble model of pulsed discharge in water," *J. Appl. Phys.* **102**(6), 063302 (2007).